



Synthesis of biodegradable pentaarmed star-block copolymers via an asymmetric BIS-TRIS core by combination of ROP and RAFT: From star architectures to double responsive micelles

Jianbo Li^a, Jie Ren^{a,b,*}, Yang Cao^a, Weizhong Yuan^a

^a Institute of Nano- and Bio-polymeric Materials, School of Material Science and Engineering, Tongji University, Shanghai 200092, PR China

^b Key laboratory Advanced Civil Engineering Materials, Ministry of Education, School of Material Science and Engineering, Tongji University, Shanghai 200092, PR China

ARTICLE INFO

Article history:

Received 9 September 2009

Received in revised form

28 December 2009

Accepted 16 January 2010

Available online 25 January 2010

Keywords:

RAFT

Star-block copolymer

Double responsive micelles

ABSTRACT

Biodegradable star-shaped poly(ϵ -caprolactone) and poly(ϵ -caprolactone-*b*-L-lactide) (5sPCL-*b*-PLLA) with five arms were synthesized by ring-opening polymerization (ROP) from an asymmetric BIS-TRIS core via “core-first” strategy. Subsequently, a series of amphiphilic and double responsive star-block copolymers were synthesized by Z-RAFT star polymerization of *N,N*-dimethylamino-2-ethyl methacrylate (DMAEMA) from the star-shaped macro-RAFT agent, which was prepared by attaching 3-benzyl-sulfanythiocarbonylthiocarbonylsufanylpropionic acid (BSPA) to 5sPCL-*b*-PLLA using a simple two-step reaction sequence. GPC and ¹H NMR data demonstrated the polymerization courses are under control. The molecular weight of 5sPCL-*b*-PLLA-*b*-DMAEMA increased with the monomer conversion, and the molecular weight distribution was in the range of 1.19–1.37. The spherical micelles with degradable core and pH/thermo-double sensitive shell had been prepared from the aqueous medium of the amphiphilic star-shaped copolymers by dialysis method. Both pH and thermal-responsive behaviours of copolymer micelles obtained in this study were investigated. The micelle size and morphology were measured by DLS, AFM and TEM.

© 2010 Elsevier Ltd. All rights reserved.

1. Introduction

Recently, considerable interests have been attracted by the biomedical materials, especially by the intelligent polymeric micelles due to their unique core-shell structures [1,2]. It is well known that core-shell type of polymeric micelles can self-assemble from amphiphilic copolymers by hydrophobic segment self-aggregation and hydrophilic segment contacting with water medium [3]. So far, most of the previously reported polymeric micelles with core-shell structure have been prepared by linear block copolymers [4], random copolymers [5], or graft copolymers [6]. However, several star-shaped copolymers were also reported to prepare core-shell micelles in recent years [7–10]. Amphiphilic star-shaped copolymers with several or a large number of linear arms are becoming attractive because it may overcome or partially

overcome the problem of thermodynamic instability associated with micelles assembled from linear copolymers [10–12].

Star polymers have been gained great attention over the past decades due to their unique three-dimensional shape and properties. This has provoked considerable interest in the preparation of a variety of star copolymers with varying arm numbers, chemical composition, and chain topology [13]. Star polymers can be produced either by “arm-first” or “core-first” methods. The “arm-first” method means to prepare the arms of linear polymer chains primarily and subsequently react with appropriate terminators or coupling agents to form the star polymers. Therefore, the resulting star polymers generally have a statistical distribution of the number of arms by the “arm-first” technique [14]. In the “core-first” method, polymer chains are propagated from a multifunctional initiator. Generally, the latter method is more popular because of better control. The arm number of a star polymer is determined by the number of end groups in the core molecule. Till now, star polymers with several arms (arm number <10) and a larger number of arms (arm numbers >10) have been reported in a pack of papers mostly with the “core-first” strategy [13,15–20]. However, the synthesis for well-defined star copolymers, especially star-block copolymers, have not grown easier until living/

* Corresponding author at: Institute of Nano- and Bio-polymeric Materials, School of Material Science and Engineering, Siping Road 1239, Tongji University, Shanghai, PR China, 200092. Tel./fax: +86 21 65989238.

E-mail address: renjie@tongji.edu.cn (J. Ren).

controlled free radical polymerization techniques were developed, such as reversible addition fragmentation chain transfer (RAFT) polymerization [15], atom transfer radical polymerization (ATRP) [20,21], and nitroxide mediated radical polymerization (NMP) [22]. Additionally, the combinations of the living/controlled radical polymerizations and their combinations with living ring-opening polymerization (ROP) have also been employed for the preparation of star copolymers [13,23].

Stimuli-responsive polymers that undergo phase transitions in response to external stimuli, such as temperature, pH, ionic strength, light or photochemical process, have been widely investigated in various fields [24,25]. In particular, many studies are focused on temperature and pH-responsive designed materials able to respond in a physiological environment. The most thoroughly investigated thermoresponsive polymers contain polyethylene glycol (PEG), oligoethylene glycol (OEG), poly(*N*-isopropylacrylamide) (PNIPAAm), or poly(*N,N*-dimethylamino-2-ethyl methacrylate) (PDMAEMA) units [26]. Of these polymers, PDMAEMA has been widely investigated and used in drug delivery systems and modification of biomedical polymer surfaces due to its biocompatibility, pH/temperature double responsiveness [27–29]. Many polymerization techniques are described to synthesize PDMAEMA including anionic polymerization and group transfer polymerization [30,31]. Concerning the controlled radical polymerizations, atom transfer radical polymerization (ATRP) of DMAEMA has been investigated to afford well-controlled polymers. For example, Sui et al. reported the homogeneous grafting of underivatized cellulose with DMAEMA via ATRP under mild conditions [28]. Yuan et al. synthesized the well-defined dendritic star copolymers by ATRP of DMAEMA with star-shaped macroinitiator [19]. However, the copper catalyst involved in ATRP of DMAEMA was complexed by amino groups in both monomer and polymer, which may lead to a loss of control over the polymerization [29,32]. In addition, the complete removal of the copper residues from the polymer products of ATRP has always been problematic. It was argued that it was important to remove the metal residue from the products particularly for biomedical applications as they may be harmful for human health. Therefore, reversible addition fragmentation chain transfer (RAFT) polymerizations was also investigated to synthesize well-controlled PDMAEMA [29,33]. When aiming at star polymer via RAFT polymerization, a star-shaped RAFT agent needs to be used, in which the stabilizing Z-group is linked to the core. This so-called Z-RAFT star polymerization effectively prevents extensive coupling reactions between star polymers as well as side-production of linear material, which occur when attaching the RAFT agent via its leaving R-group to the core [34,35]. The RAFT agent used in this paper for this purpose is 3-benzylsulfanylthiocarbonylthiocarbonylsufanylpropionic acid (BSPA), which is attached to the star core via a simple two-step reaction sequence. It is clear that the use of the trithiocarbonate BSPA in conjunction with AIBN allows for the synthesis of PDMAEMA in a controlled fashion [33]. Such trithiocarbonates have been previously shown to be effective for the controlled polymerization of a variety of monomers [18,34,36].

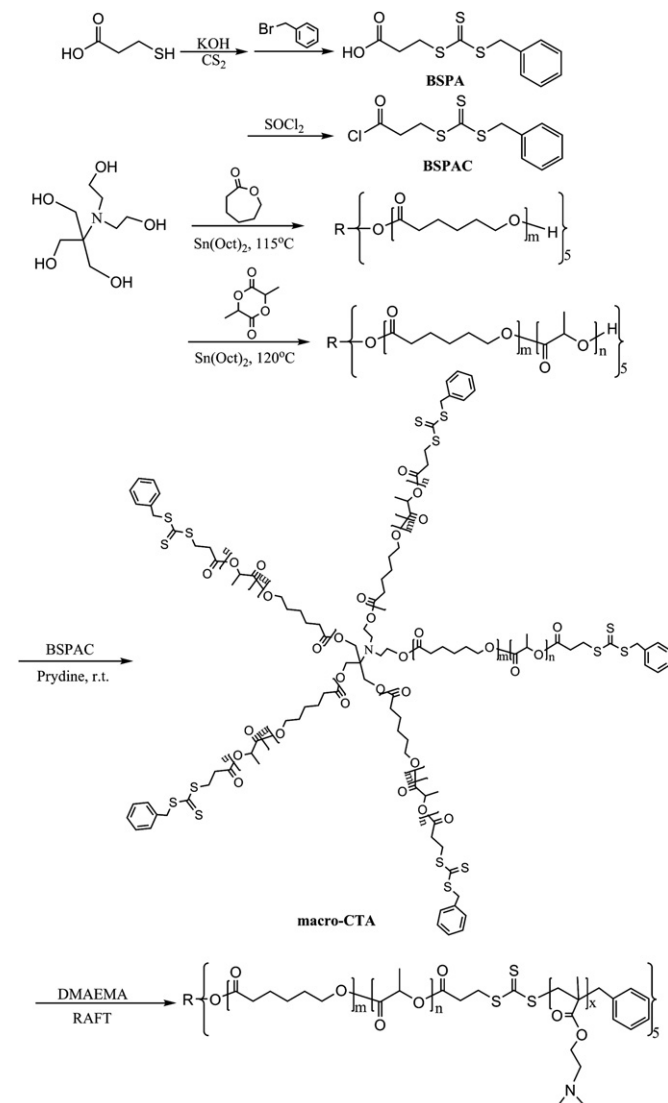
On the other hand, poly(lactide) (PLA) and poly(ϵ -caprolactone) (PCL) are biodegradable and biocompatible linear polyesters with good mechanical properties, low immunogenicity and FDA approval [37,38]. They have been widely adopted for biomaterials and biomedical applications. So PLA and PCL usually were selected as hydrophobic blocks of amphiphilic copolymers to form hydrophobic cores of the core-shell type of polymeric micelles, working as the sustained release reservoir of insoluble or unstable drug molecules [3,39]. In the present work, we first started to explore the utilization of bis(2-hydroxyethyl)amino-tris(hydroxymethyl)-methane (BIS-TRIS), a buffering agent with five hydroxyl groups usually used in biochemistry, as multifunctional cores for ring-

opening polymerization. We aimed to synthesize a series of novel amphiphilic and biocompatible star-block copolymers with pH/thermo-double sensitiveness by combination of ROP and RAFT polymerization from an asymmetric multifunctional core. A star-shaped hydroxyl-terminated PCL with five arms was firstly synthesized by ROP with BIS-TRIS as multifunctional initiator. Subsequently, the terminal hydroxyl groups of star-shaped PCL are used to initiate the ROP of *L*-lactide and then reacted with 3-benzylsulfanylthiocarbonylsufanylpropionic acid chloride (BSPAC) to produce the macro-chain transfer agent (macro-CTA, 5sPCL-*b*-PLLA-BSPA) for the subsequent RAFT polymerization (Scheme 1). In the structure of the novel star-block copolymer, biodegradable and hydrophobic PCL-*b*-PLLA blocks can self-aggregate in the core while PDMAEMA blocks serve as stimuli-responsive and hydrophilic segments that form the outer shell of polymeric micelles.

2. Experimental

2.1. Materials

ϵ -Caprolactone (ϵ -CL; Acros Organic, USA) was purified with CaH_2 by vacuum distillation. *L*-lactide (L-LA; TJL Biomaterials,



Scheme 1. Synthesis of the star-block amphiphilic copolymer by ring-opening polymerization and RAFT polymerization.

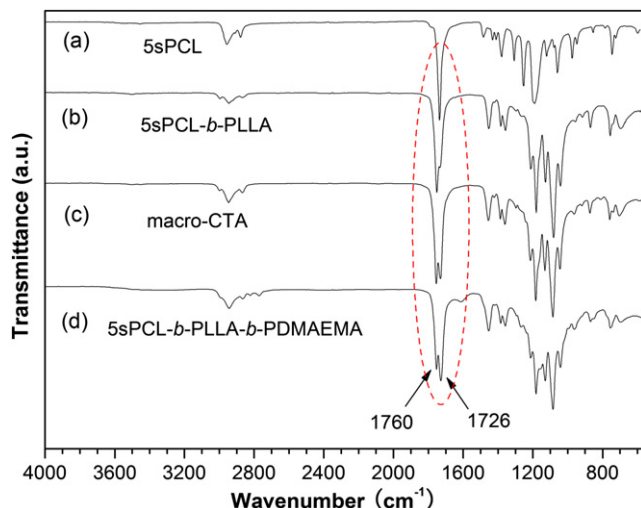


Fig. 1. FT-IR spectra of (a) 5sPCL star polymer, (b) 5sPCL-b-PLLA star-diblock copolymer, (c) macro-CTA 5sPCL-b-PLLA-BSPA, and (d) 5sPCL-b-PLLA-b-PDMAEMA star-tri-block copolymer.

Shanghai) was purified by twice recrystallization from ethyl acetate and dried in a vacuum at room temperature. Tin 2-ethylhexanoate ($\text{Sn}(\text{Oct})_2$; Aldrich, USA) was distilled under reduced pressure before use. Bis(2-hydroxyethyl)amino-tris(hydroxymethyl)methane (BIS-TRIS; Aladdin-Reagent, Shanghai) was dried at 60°C *in vacuo* for 24 h before use. *N,N*-dimethylamino-2-ethyl methacrylate (DMAEMA; Acros Organics, USA) was also dried over CaH_2 and distilled under reduced pressure. Azobisisobutyronitrile (AIBN; SCRC, Shanghai) were purified by twice recrystallization from ethanol. 3-Mercaptopropionic acid (99%; AlfaAesar, USA) and benzyl bromide ($\geq 99\%$; Aladdin-Reagent, Shanghai) were used without further purification. Thionyl chloride was distilled before use. Pyridine and 1,4-dioxane were dried over CaH_2 and distilled before use. Carbon disulfide ($>99\%$) and all other chemicals obtained from Sinopharm Chemical Reagent Company (SCRC) were of analytical grade and were used as received.

2.2. Characterization

Attenuated total reflection Fourier transform infrared (ATR FT-IR) spectra were recorded on an AVATAR 360 ESP FT-IR spectrometer. ^1H NMR spectra were obtained using a Bruker DMX-500 NMR spectrometer with CDCl_3 or D_2O as solvent at 25°C . The chemical shifts were relative to tetramethylsilane (TMS) at $\delta = 0$ ppm for protons. The average molecular weight and its distribution were determined using a gel permeation chromatographic (GPC) system equipped with a Waters 150 C separations module and a Waters differential refractometer. Polymer samples were dissolved in THF at a concentration of 1–2 mg/mL. THF was eluted at 1.0 mL/min through two Waters Styragel HT columns and a linear column. The internal and column temperatures were kept constant at 35°C . The molecular weights were calculated against polystyrene standards. The measurements of static contact angles were carried out by commercial contact angle analysis instruments (OCA 20, DataPhysics, Germany). A distilled water droplet of 3 μL was used as the indicator. The films with thickness of $\sim 120\ \mu\text{m}$ were obtained by casting polymer solutions on the clean glass slides using chloroform as a solvent, followed by slow solvent evaporation at room temperature for about one day. Optical transmittance of aqueous polymer solutions at various temperatures or pH was measured at $\lambda = 500\ \text{nm}$ using a Hitachi U-3310 UV-VIS spectrophotometer. The temperature of the sample cell was

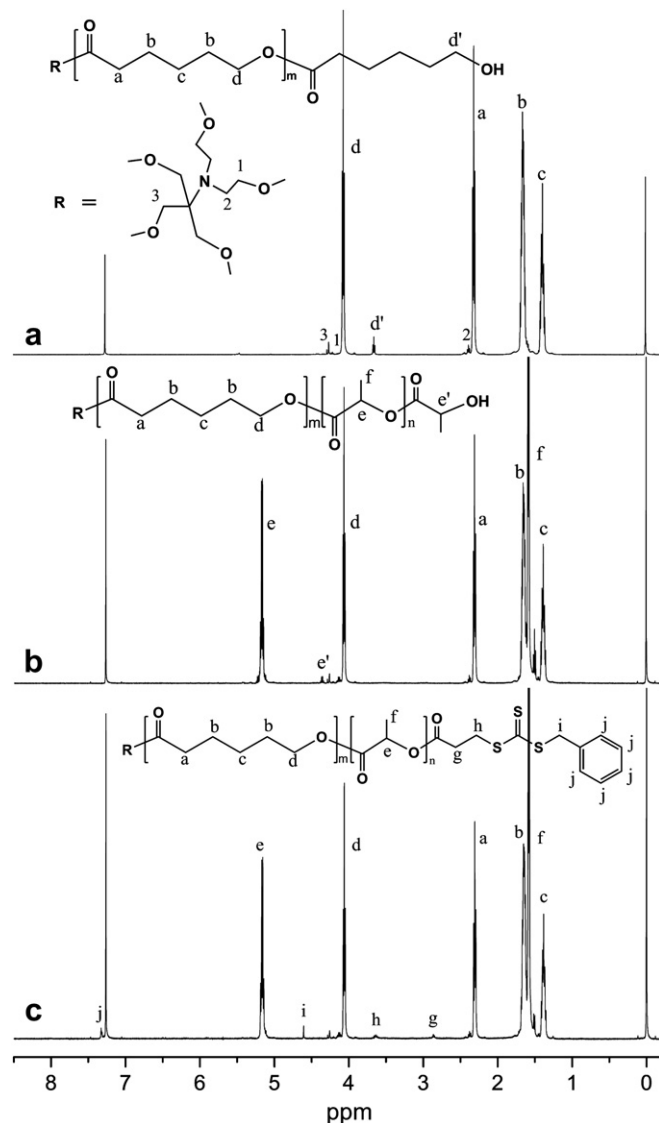


Fig. 2. ^1H NMR spectra of (a) 5sPCL star polymer, (b) 5sPCL-b-PLLA star-block copolymer, (c) macro-CTA 5sPCL-b-PLLA-BSPA.

thermostatically controlled using an electronic thermostatic cell holder and a temperature controller; the heating rate was set at $0.5^\circ\text{C}/\text{min}$. The LCST (lower critical solution temperature) value of the polymer solution was defined as the temperature producing a 50% decrease in optical transmittance [4].

Table 1
Preparation of star polymer 5sPCL and star-block copolymer 5sPCL-b-PLLAs.

Sample	[CL]/[OH]	[LLA]/[OH]	$M_{n,\text{th}}^a$	$M_{n,\text{NMR}}^b$	$M_{n,\text{GPC}}^c$	M_w/M_n^c	Conversion (%) ^d
1	20:1		11,400	12,190	11,060	1.27	98.1
2		10:1	17,920	18,790	17,100	1.23	95.2
3		20:1	25,300	27,500	24,760	1.11	96.9
4		30:1	31,530	33,270	30,450	1.29	94.7
5		40:1	37,750	39,860	36,500	1.28	92.6

^a $M_{n,\text{th}} = [\text{monomer}]/[\text{OH}] \times 5 \times M_{\text{monomer}} \times \text{Conversion} (\%) + M_{\text{initiator}}$; $M_{n,\text{th}}$ denotes the number-average molecular weight of star-shaped polymer.

^b Determined by ^1H NMR spectroscopy of star-shaped polymer.

^c Determined by GPC analysis with polystyrene standards. THF was used as eluent.

^d Conversion of monomer obtained from gravimetry.

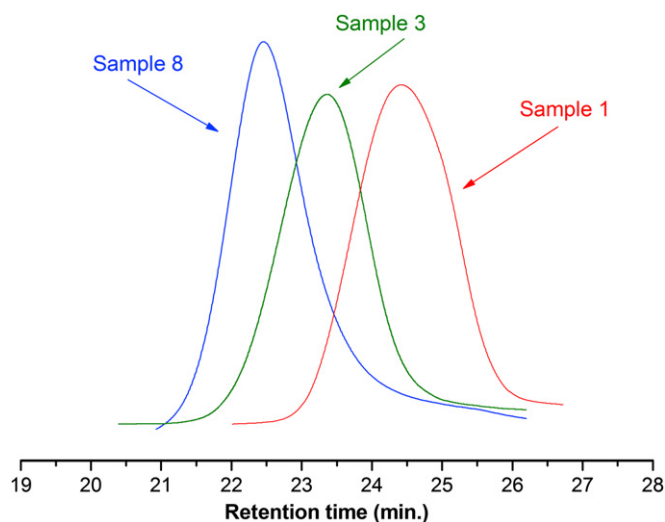


Fig. 3. GPC traces of 5sPCL star polymer (Sample 1), 5sPCL-*b*-PLLA star-diblock copolymer (Sample 3), and 5sPCL-*b*-PLLA-*b*-PDMAEMA star-triblock copolymer (Sample 8).

2.3. Preparation

2.3.1. Synthesis of 3-benzylsulfanylthiocarbonylsufanylpropionic acid (RAFT acid)

The RAFT agent, 3-benzylsulfanylthiocarbonylsufanylpropionic acid (BSPA) was synthesized according to the literature [18] with minor modification. 3-Mercaptopropionic acid (20 mL, 0.23 mol) was slowly added into a solution of potassium hydroxide (26 g, 0.46 mol) in 250 mL of water. And carbon disulfide (30 mL) was added dropwise into the solution for more than 40 min with vigorous stirring, and the solution was further stirred for 8 h. After that, benzyl bromide (39.6 g, 0.23 mol) was added into the solution, and then the reaction mixture was heated for 12 h at 80 °C. After cooling and the addition of chloroform (300 mL), the reaction mixture was acidified with hydrochloric acid until the organic layer became yellow. The water phase was extracted with chloroform (2 × 100 mL). The combined organic layers were washed with 100 mL of saturated sodium chloride and then with 100 mL of water twice and finally dried over anhydrous magnesium sulfate overnight. After evaporation of the solvent, the remaining product was recrystallized in dichloromethane three times, and 52 g of yellow solid with a yield of 83% was obtained.

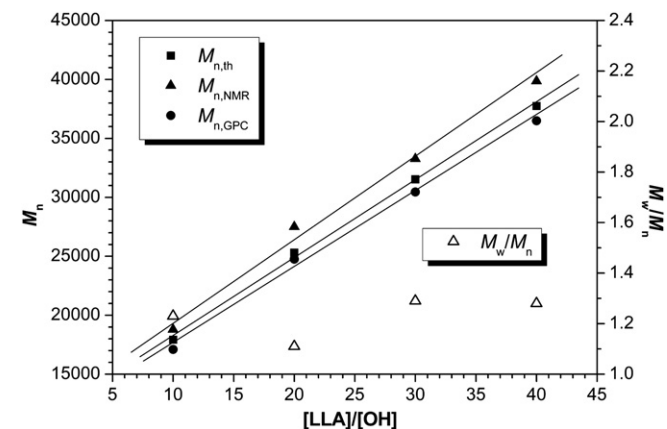


Fig. 4. Dependence of M_n and M_w/M_n on the molar ratio of [LLA]/[OH] with 5sPCL star polymer initiator (sample 1) and tin 2-ethylhexanoate catalyst in bulk at 120 °C.

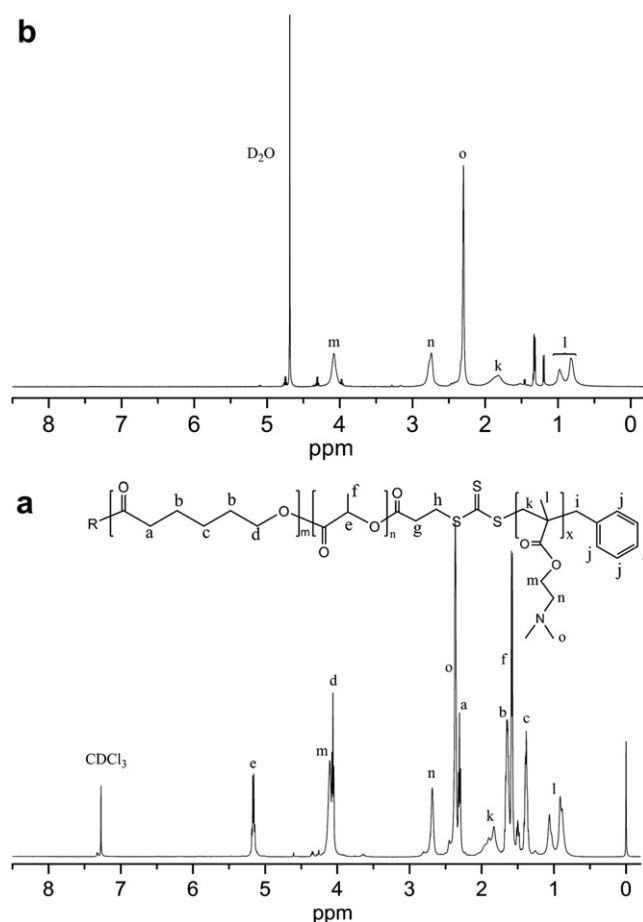


Fig. 5. ¹H NMR spectra of (a) 5sPCL-*b*-PLLA-*b*-PDMAEMA star-triblock copolymer in CDCl₃ and (b) micelles formed by the star-triblock copolymer in D₂O.

¹H NMR (CDCl₃, δ , ppm): 10.1 (b, 1H, –COOH), 7.32–7.25 (m, 5H, –Ph), 4.61 (s, 2H, –CH₂Ph), 3.61 (t, 2H, –CH₂S), 2.84 (t, 2H, –CH₂C=O).

2.3.2. Synthesis of 3-benzylsulfanylthiocarbonylsufanylpropionic acid chloride (BSPAC)

BSPA (5.0 g, 0.18 mol) and 20 mL of anhydrous dichloromethane were introduced into a dried flask with a magnetic stirring bar. Freshly distilled thionyl chloride (5 mL) was added dropwise to the BSPA mixture solution over 30 min. The mixture was then gradually warmed and refluxed until a clear solution was obtained. After another hour of refluxing, the product was isolated by evaporation

Table 2

RAFT polymerization of DMAEMA with 5sPCL-*b*-PLLA-BSPA^a as macro-CTA. (Polymerization condition: [macro-CTA] = 0.2 × 10^{−2} mol/L; [macro-CTA]:[AIBN] = 2:1; [DMAEMA] = 1.5 mol/L; temperature: 80 °C; solvent: dioxane).

Sample	Time (h)	$M_{n,th}^b$	$M_{n,NMR}^c$	$M_{n,GPC}^d$	M_w/M_n^d	Conversion (%) ^e
6	1	32,850	33,900	30,420	1.19	5.9
7	2	36,860	38,250	35,190	1.26	9.3
8	4	43,350	45,630	40,830	1.21	14.8
9	6	47,800	49,750	43,260	1.35	18.6
10	8	50,300	52,180	47,600	1.37	20.7

^a $M_{n,macro-CTA}$ (5sPCL-*b*-PLLA-BSPA) = 25,900, M_w/M_n = 1.15.

^b $M_{n,th} = [DMAEMA]/[macro-CTA] \times M_{DMAEMA} \times \text{Conversion} (\%) + M_{n,macro-CTA}$; $M_{n,th}$ denotes the number-average molecular weight of star-shaped copolymer.

^c Determined by ¹H NMR spectroscopy of star-shaped copolymer.

^d Determined by GPC analysis with polystyrene standards. THF was used as eluent.

^e Conversion of monomer obtained from gravimetry.

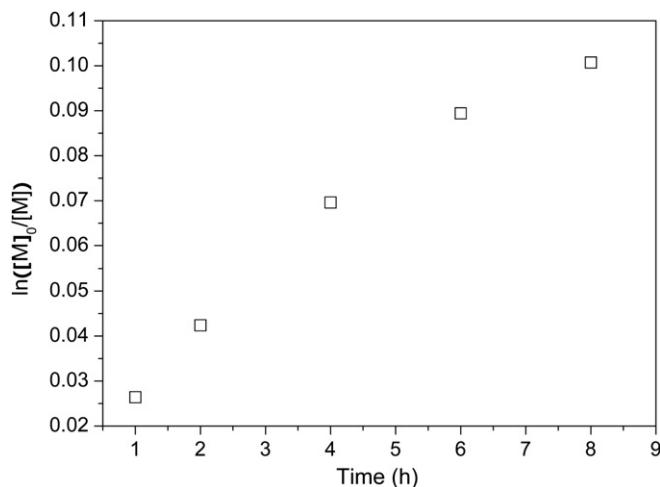


Fig. 6. Semilogarithmic plot of monomer consumption versus time for the RAFT polymerization of DMAEMA using macro-CTA as the RAFT agent in dioxane.

of the solvent with vacuum distillation. The remaining yellow oil was dried under a high vacuum. The product was used immediately for the next synthesis.

^1H NMR (CDCl_3 , δ , ppm): 7.32–7.26 (m, 5H, –Ph), 4.61 (s, 2H, $-\text{CH}_2\text{Ph}$), 3.61 (t, 2H, $-\text{CH}_2\text{S}$), 3.34 (t, 2H, $-\text{CH}_2\text{C}=\text{O}$).

2.3.3. Synthesis of the hydroxyl-terminated star-shaped poly(ϵ -caprolactone) (5sPCL)

The hydroxyl-terminated star-shaped poly(ϵ -caprolactone) (5sPCL) was synthesized by ring-opening polymerization of CL with BIS-TRIS as initiator. Briefly, CL (15 g, 131.4 mmol), BIS-TRIS (0.275 g, 1.314 mmol) and a catalytic amount of $\text{Sn}(\text{Oct})_2$ were added to a flame-dried polymerization tube quickly. The tube was then connected to a Schlenk line, where evacuating–refilling processes were repeated for three times. Then, the tube was put into an oil bath at 115°C under nitrogen atmosphere with stirring and cooled to room temperature after polymerization for 24 h. The crude polymer was dissolved in chloroform and precipitated two times in methanol. The purified polymer was dried in a vacuum oven at room temperature until a constant weight.

Number-average molecular weight determined by ^1H NMR ($M_{n,\text{NMR}}$): 12,190. Number-average molecular weight determined by GPC ($M_{n,\text{GPC}}$): 11,060. Weight-average molecular weight/number-average molecular weight (M_w/M_n): 1.27. IR (cm^{-1}): 3430–

3560 ($\nu_{\text{O-H}}$), 2948 ($\nu_{\text{C-H}}$), 2869 ($\nu_{\text{C-H}}$), 1730 ($\nu_{\text{C=O}}$), 1472 ($\nu_{\text{C-H}}$), 1245 ($\nu_{\text{C-O}}$). ^1H NMR (CDCl_3 , δ , ppm): 4.21–4.25 (m, CH_2OH in BIS-RIS), 4.06 (m, CH_2O in PCL), 3.65 (t, terminal CH_2O in PCL), 2.37 (m, NCH_2 in BIS-RIS), 2.31 (m, COCH_2 in PCL), 1.65 (m, CH_2 in PCL), 1.38 (m, CH_2 in PCL).

2.3.4. Synthesis of the hydroxyl-terminated star-diblock copolymers (5sPCL-*b*-PLLA)

A typical polymerization procedure was as follows: The hydroxyl-terminated 5sPCL (4.25 g, 0.384 mmol, containing 1.92 mmol of $-\text{OH}$ groups), L-LA (5.54 g, 38.43 mmol), and a dried magnetic stirring bar were added to a fire-dried polymerization tube quickly. The tube was then connected to a Schlenk line, where evacuating–refilling processes were repeated three times. The tube was put into an oil bath at 120°C with vigorous stirring for 5 min. A catalytic amount of $\text{Sn}(\text{Oct})_2$ in anhydrous toluene was added to the melted mixture, and the evacuating–refilling process was carried out again to remove the toluene. The tube was put into an oil bath at 120°C under nitrogen atmosphere with stirring and cooled to room temperature after polymerization for 24 h. The resulting product was dissolved in chloroform and precipitated two times with methanol. The purified polymer was dried in a vacuum oven at room temperature until constant weight.

IR (cm^{-1}): 3430–3560 ($\nu_{\text{O-H}}$), 2948 ($\nu_{\text{C-H}}$), 2865 ($\nu_{\text{C-H}}$), 1760 ($\nu_{\text{C=O}}$), 1726 ($\nu_{\text{C=O}}$), 1453 ($\nu_{\text{C-H}}$), 1245 ($\nu_{\text{C-O}}$). ^1H NMR (CDCl_3 , δ , ppm): 5.18 (m, CHO in PLLA), 4.38 (m, terminal CHO in PLLA), 4.12–4.27 (m, CH_2OH in BIS-RIS), 4.07 (m, CH_2O in PCL), 2.38 (m, NCH_2 in BIS-RIS), 2.31 (m, COCH_2 in PCL), 1.65 (m, CH_2 in PCL), 1.59 (m, CH_3 in PLLA), 1.51 (m, terminal CH_3 in PLLA), 1.39 (m, CH_2 in PCL).

2.3.5. Synthesis of macro-chain transfer agent (macro-CTA, 5sPCL-*b*-PLLA-BSPA)

Dried 5sPCL-*b*-PLLA (Sample 3) (13.75 g, 0.5 mmol, containing 2.5 mmol of $-\text{OH}$ groups) and anhydrous pyridine (0.784 g, 10 mmol) were dissolved into 80 mL of dried methylene chloride at room temperature. The mixture was stirred and cooled to 0°C . Then, excess BSPAC (2.92 g, 10 mmol) in 20 mL of dried methylene chloride was added dropwise to the mixture within 40 min. After stirring at room temperature for 12 h, the solution was extracted three times with 50 mL of water. The organic phase was dried over anhydrous sodium sulfate for 5 h, and filtered. The filtrate was concentrated and then precipitated two times with methanol. The resulting product was dried *in vacuo* at room temperature in the yield of 86% and stored in a sealed bottle in a cool and dark place.

$M_{n,\text{NMR}} = 28,700$, $M_{n,\text{GPC}} = 25,900$, $M_w/M_n = 1.15$. IR (cm^{-1}): 2948 ($\nu_{\text{C-H}}$), 2865 ($\nu_{\text{C-H}}$), 1760 ($\nu_{\text{C=O}}$), 1726 ($\nu_{\text{C=O}}$), 1453 ($\nu_{\text{C-H}}$), 1245 ($\nu_{\text{C-O}}$). ^1H NMR (CDCl_3 , δ , ppm): 7.32–7.27 (m, 5H, –Ph), 5.18 (m, CHO in PLLA), 4.62 (s, 2H, $-\text{CH}_2\text{Ph}$), 4.07 (m, CH_2O in PCL), 3.61 (t, 2H, $-\text{CH}_2\text{S}$), 2.84 (t, 2H, $-\text{CH}_2\text{C}=\text{O}$), 2.31 (m, COCH_2 in PCL), 1.65 (m, CH_2 in PCL), 1.58 (m, CH_3 in PLLA), 1.38 (m, CH_2 in PCL).

2.3.6. Synthesis of the star-triblock copolymers (5sPCL-*b*-PLLA-*b*-PDMAEMA)

The 5sPCL-*b*-PLLA-*b*-PDMAEMA star-triblock copolymers were synthesized by RAFT polymerization of DMAEMA in 1,4-dioxane with 5sPCL-*b*-PLLA-BSPA as macro-RAFT agent. A typical polymerization procedure was as follows: A dry Schlenk flask with magnetic stirrer was charged with DMAEMA (2.358 g, 15 mmol), the star-shaped macro-RAFT agent (5sPCL-*b*-PLLA-BSPA) (0.574 g, 0.02 mmol, containing 0.1 mmol of BSPA groups), AIBN (16.4 mg, 0.01 mmol), and 10 mL of dried 1,4-dioxane. The flask was degassed with three freeze–evacuate–thaw cycles at the temperature of liquid nitrogen. After the polymerization was performed at 80°C for 4 h, the flask was cooled for half an hour in an ice bath and precipitated in 250 mL of diethyl ether for two times. The

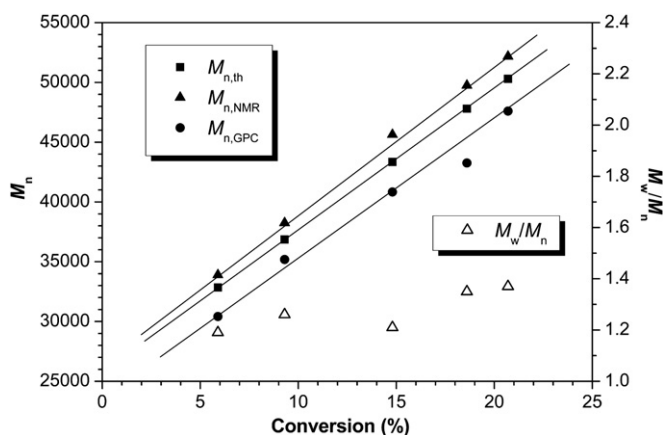


Fig. 7. Dependence of M_n and M_w/M_n of the star-triblock copolymer 5sPCL-*b*-PLLA-*b*-PDMAEMA on the conversion of the monomer DMAEMA.

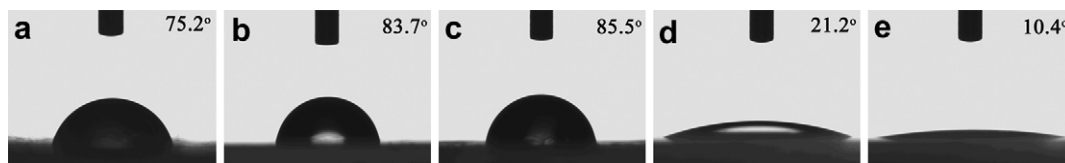


Fig. 8. Photograph of the water contact angles of a) 5sPCL (Sample 1), b) 5sPCL-b-PLLA (Sample 3), c) 5sPCL-b-PLLA-BSPA (macro-CTA), d) 5sPCL-b-PLLA-b-PDMAEMA (Sample 6), and e) 5sPCL-b-PLLA-b-PDMAEMA (Sample 10).

precipitate was filtered, and the product was dried at room temperature in a vacuum oven for 48 h to give a yield of 14.8%.

IR (cm^{-1}): 3130–3560 ($\nu_{\text{C-H}}$), 2943 ($\nu_{\text{C-H}}$), 2865 ($\nu_{\text{C-H}}$), 2767 ($\nu_{\text{C-H}}$), 1760 ($\nu_{\text{C=O}}$), 1726 ($\nu_{\text{C=O}}$), 1453 ($\nu_{\text{C-H}}$), 1245 ($\nu_{\text{C-O}}$). ^1H NMR (CDCl_3 , δ , ppm): 7.32–7.29 (m, 5H, -Ph), 5.16 (m, CHO in PLLA), 4.62 (s, 2H, -CH₂Ph), 4.09 (m, OCH₂ in PDMAEMA), 4.06 (m, CH₂O in PCL), 3.61 (t, 2H, -CH₂S), 2.84 (t, 2H, -CH₂C=O), 2.67 (m, CH₂N in PDMAEMA), 2.37 (m, NCH₃ in PDMAEMA), 2.31 (m, COCH₂ in PCL), 1.78–2.09 (m, CH₂ in PDMAEMA), 1.66 (m, CH₂ in PCL), 1.58 (m, CH₃ in PLLA), 1.38 (m, CH₂ in PCL), 0.89–1.06 (m, CH₃ in PDMAEMA).

2.4. Preparation of 5sPCL-b-PLA-b-PDMAEMA micelles

Dialysis method was used to prepare the copolymer micelles. Briefly, the star-shaped copolymer 5sPCL-b-PLA-b-PDMAEMA (100 mg) was dissolved in 4 mL of DMF. The solution was dropped into 16 mL distilled water slowly under agitation. The copolymer solution was left to stir overnight prior to dialysis against distilled water for 48 h to remove DMF using a dialysis membrane with a molecular weight cut-off of 14,000 (Sinopharm Chemical Reagent Company, Shanghai). The water was replaced hourly for the first 3 h. After dialysis, the blue aqueous solution in the dialysis bag was collected and filtered with 0.45 μm syringe filter and freeze-dried for 2 days.

2.5. Morphology characterizations of copolymer micelles (DLS, TEM and AFM)

The hydrodynamic diameter and the particle size distribution of the copolymer micelles in buffer solutions of different pH were determined by dynamic light scattering spectrophotometer (DLS, Autosizer 4700, Malvern) equipped with an argon ion laser operating at 532 nm with a fixed scattering angle of 90°. Before measurement, all samples were redispersed in buffer solutions

(pH = 1.0, 4.0, 7.0, 10.0, 12.0) to form transparent solution (2 mg/mL), sonicated for 30 s, and filtered through a 0.45 μm filter (Millipore) to remove large aggregates.

The morphology of the micelles was determined on a Transmission Electron Microscopy (TEM) (Hitachi H-600, Japan) at an accelerating voltage of 120 kV. A small drop from the aqueous copolymer solutions was deposited onto a copper grid coated with carbon film. The excess of copolymer solution was wiped off with a filter paper, and the grid was dried under ambient atmosphere for 1 h. The specimen on the copper grid was negatively stained with phosphotungstic acid.

The atom force microscopy (AFM) images of the copolymer micelles were recorded on a SPA-300HV atomic force microscope (SII NanoTechnology, Japan). The sample preparation was similar to that for TEM, but newly cleaved fresh mica surface was used as the substrate.

3. Results and discussion

3.1. Synthesis and characterization of the star-shaped poly(ϵ -caprolactone)

The star-shaped poly(ϵ -caprolactone) homopolymer was synthesized by ring-opening polymerization of CL at 115 °C. The BIS-TRIS with five hydroxyl groups was chose as the initiator in order to produce the hydroxyl-terminated star-shaped PCL. The IR spectrum of the 5sPCL is shown in Fig. 1(a). The intensive absorption peak at 1730 cm^{-1} was assigned to the carbonyl band of PCL. ^1H NMR spectrum of the star-shaped PCL is shown in Fig. 2(a). The typical signals of the methylene protons of the initiator BIS-TRIS could be clearly detected at 4.21–4.25 ppm and 2.37 ppm. The major resonance peaks (a–d) were attributed to PCL. The peak of the methylene (d) protons was detected at 4.06 ppm when the peak of the protons of the terminal methylene (d') could be discovered at

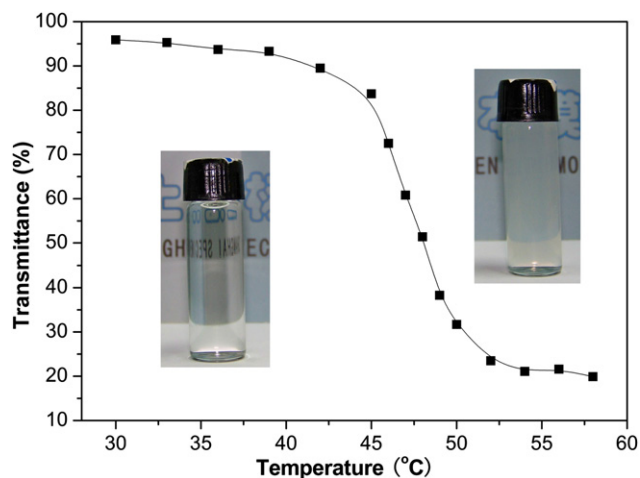


Fig. 9. Temperature dependence of optical transmittance at 500 nm for aqueous 5sPCL-b-PLLA-b-PDMAEMA (sample 8) solution with concentration of 2 mg/mL.

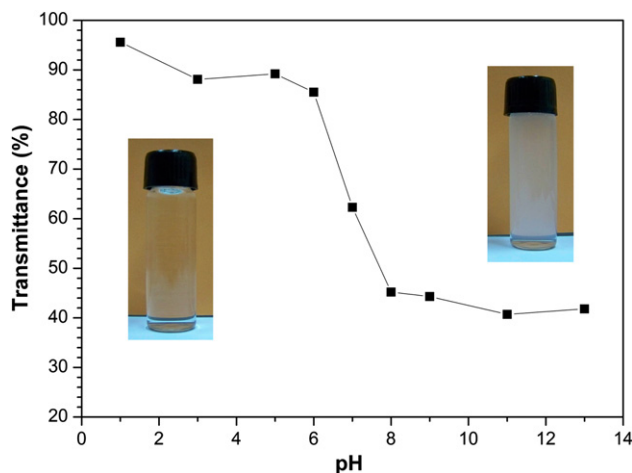


Fig. 10. pH dependence of optical transmittance at 500 nm for aqueous 5sPCL-b-PLLA-b-PDMAEMA (sample 8) solution with concentration of 10 mg/mL.

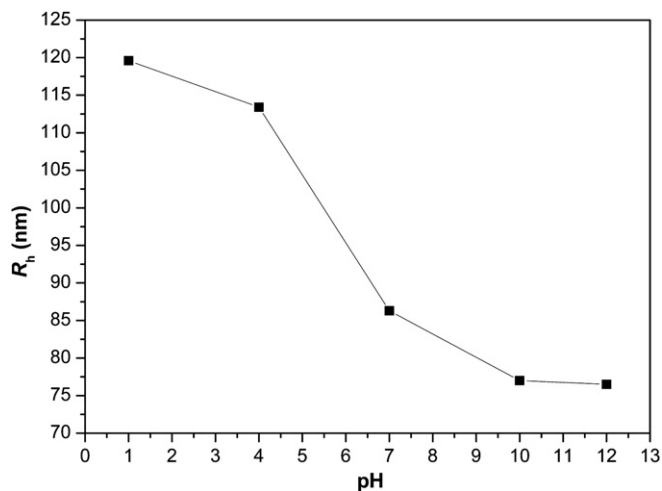


Fig. 11. pH dependence of hydrodynamic radius (R_h) of micelles formed from aqueous 5sPCL-*b*-PLLA-*b*-PDMAEMA (sample 8) solution with concentration of 2 mg/mL.

3.65 ppm which indicated that PCL was terminated by hydroxyl groups. The average degrees of polymerization for the PCL arms could be calculated from the integration ratio between the methylene protons in the repeat units (d) and those in the terminal unit (d') based on ^1H NMR spectrum. The molecular weight data of 5sPCL determined by ^1H NMR spectrum and GPC analysis were listed in Table 1. The GPC trace of 5sPCL (Sample 1) is shown in Fig. 3. It could be seen that the trace was monomodal, which indicated that the sample was pure star-shaped PCL homopolymer. All these demonstrated that well-defined 5-arm star-shaped PCL with narrow number-average molecular weight distributions could be successfully synthesized by ROP of CL with BIS-TRIS initiator.

3.2. Synthesis and characterization of the star-diblock 5sPCL-*b*-PLLA copolymers

The 5sPCL-*b*-PLLA star-diblock copolymers were synthesized by the reaction of hydroxyl-terminated star-shaped PCL with L-LA at 120 °C with bulk polymerization. The IR spectrum of the 5sPCL-*b*-PLLA star-diblock copolymer is shown in Fig. 1(b). The main difference in the IR spectrum between 5sPCL-*b*-PLLA and 5sPCL was the carbonyl absorption band region. In the IR spectrum of 5sPCL-*b*-PLLA, the carbonyl absorption band became wide and split into two peaks. The peak at 1760 cm^{-1} corresponded to the carbonyl absorption of PLLA units, while the peak at 1726 cm^{-1} was assigned to the carbonyl absorption of PCL units. It was important to prove that the PLLA chains existed in the copolymer as a block [17]. The ^1H NMR spectrum of 5sPCL-*b*-PLLA is shown in Fig. 2(b). The peak assigned to the methylene protons of the PCL block at 3.65 ppm disappeared, and a new peak at 4.38 ppm for the produced end group of the PLLA block was observed. This indicated that the terminal hydroxyl groups of the 5sPCL macroinitiator successfully initiated the polymerization of L-LA.

The average polymerization degree of L-LA was also determined by the integration ratio of methine protons of the PLLA block at 4.38 ppm and the methylene protons of PCL at 2.31 ppm. As shown in Table 1 and Fig. 4, the number-average molecular weight of the resulting copolymers linearly increased with the molar ratio of monomer to macroinitiator, which indicated that the hydroxyl-terminated star-shaped polyester could be used as effective propagation centers and all of the five hydroxyl groups of the star-shaped polyester molecule could initiate the ROP of L-LA. In addition, the number-average molecular weight distributions of these polymers were narrow ($1.11 \leq M_w/M_n \leq 1.29$). The GPC trace of the

star-diblock copolymer 5sPCL-*b*-PLLA (sample 3) is shown in Fig. 3. These trace was comparatively symmetrical and monomodal, suggesting that these purified polymers were pure homopolymer or star-block copolymers.

3.3. Synthesis and characterization of the macro-chain transfer agent (macro-CTA) and star-triblock 5sPCL-*b*-PLLA-*b*-PDMAEMA copolymers

The star-shaped 5sPCL-*b*-PLLA-BSPA macro-RAFT agent was obtained by the reaction of 5sPCL-*b*-PLLA with BSPAC. The molecular weight of 5sPCL-*b*-PLLA-BSPA increased slightly and the molecular weight distribution was similar to that of 5sPCL-*b*-PLLA. In IR spectrum (Fig. 1(c)), the peak at 1726 cm^{-1} corresponding to the carbonyl absorption of PCL units and terminal BSPAs became slightly intensive, which could be used to prove that the BSPA molecules existed in the copolymer as a terminal unit. ^1H NMR spectrum was shown in Fig. 2(c). The signal at 4.38 ppm disappeared, while novel signals corresponding to methylene protons (g, h, i) and phenyl protons (j) of terminal BSPAs appeared at 2.84 ppm, 3.61 ppm, 4.62 ppm, and 7.32–7.27 ppm, indicating that all the terminal hydroxyl groups have been reacted completely.

Star-triblock 5sPCL-*b*-PLLA-*b*-PDMAEMA copolymer was prepared from 5sPCL-*b*-PLLA-BSPA macro-CTA and DMAEMA via RAFT at 80 °C. According to the IR spectrum shown in Fig. 1(d), the carbonyl absorption band became wide and split into two peaks obviously. The peak at 1760 cm^{-1} corresponded to the carbonyl absorption of PLLA units, while the peak at 1726 cm^{-1} was assigned to the superposition of carbonyl absorption of PDMAEMA units, PCL units, and BSPA units. ^1H NMR spectrum of the copolymer is shown in Fig. 5(a). All the protons signals of the copolymer could be detected. The degree of polymerization of the DMAEMA block was obtained from the integration of the proton signals at 5.16 ppm (e in PLLA block) and 2.67 ppm (n in PDMAEMA block). The GPC trace of the amphiphilic star copolymer is shown in Fig. 3 (Sample 8). It could be seen that the trace was monomodal but showed a small tailing toward the low molecular weight. Furthermore, according to the data given in Table 2, the molecular weights determined by GPC ($M_{n,\text{GPC}}$) were much lower than those determined by ^1H NMR ($M_{n,\text{NMR}}$) and theoretic values ($M_{n,\text{th}}$). Since GPC operates on the principal of hydrodynamic volume of the polymer in solvent, it is often incorrect for highly branched polymers such as star polymers. The most important characteristic of star polymers is their high segment density in comparison to their linear homologs of the same molecular weight. This implies that star polymers exhibit a smaller hydrodynamic volume, which leads to higher elution volumes in certain time frame in a size exclusion chromatography apparatus. It means that the apparent molecular weight of such species, as obtained from standard GPC calibrated with well-defined linear homologs, are lower than their real molecular weight [40,41]. In addition, the absorption of PDMAEMA onto the GPC column also resulted in an increase of retention time detected by GPC and led to the tailing phenomenon of GPC trace [42,43].

The polymerization kinetics of DMAEMA using macro-CTA as the RAFT agent was studied. The monomer conversion was determined by weighing the samples. Semilogarithmic plot of the monomer conversion of DMAEMA versus the reaction time is shown in Fig. 6. The conversion of DMAEMA reached 20.7% at 8 h in dioxane. The plot of $\ln([M]_0/[M])$ increased nearly linearly with the reaction time as expected for a controlled polymerization, which suggests that most of the 5sPCL-*b*-PLLA-BSPA macro-CTA retained the trithiocarbonate functionality at the chain terminus and that it was available for subsequent reactivation. It could be seen from Fig. 7 that $M_{n,\text{NMR}}$ values were close to $M_{n,\text{th}}$, increased linearly with conversion, indicating that the molecular weight of the star

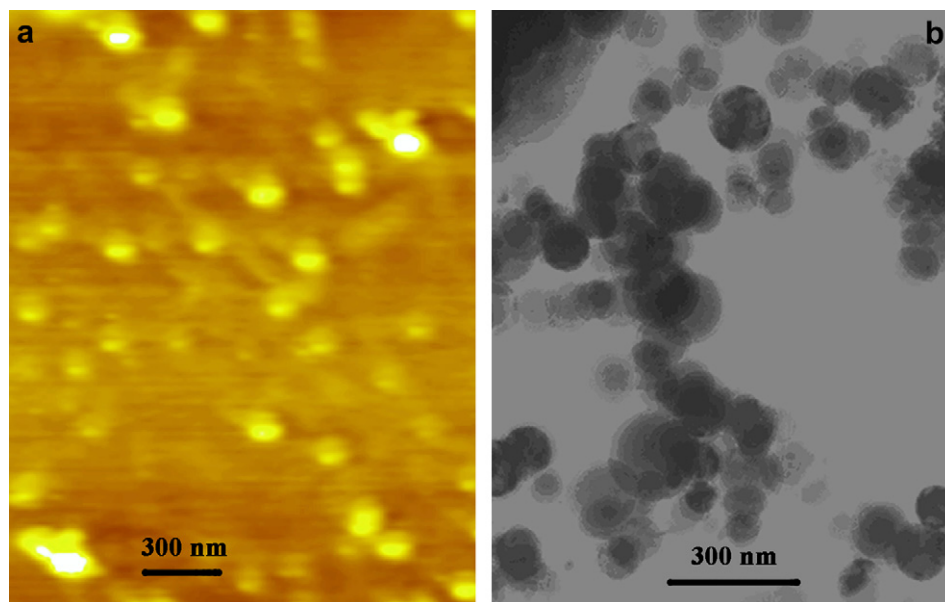


Fig. 12. (a) AFM and (b) TEM images of the micelles formed from aqueous 5sPCL-*b*-PLLA-*b*-PDMAEMA (sample 8) solution at pH = 7.

copolymer could be manipulated by the control of monomer conversion. Moreover, the molecular weight distributions of the copolymers were narrow ($M_w/M_n \leq 1.37$) and increase at higher conversions. Obviously, the star-shaped 5sPCL-*b*-PLLA-BSPA could be used as an efficient macro-RAFT agent for living polymerization of DMAEMA to form amphiphilic star-block copolymer 5sPCL-*b*-PLLA-*b*-PDMAEMA.

3.4. Hydrophilicity investigation of polymers

The hydrophilicity of the films prepared from 5sPCL, 5sPCL-*b*-PLLA, 5sPCL-*b*-PLLA-BSPA, and 5sPCL-*b*-PLLA-*b*-PDMAEMA was measured with water contact angles. As shown in Fig. 8, the contact angle of the 5sPCL surface was 75.2°. The contact angle of the 5sPCL-*b*-PLLA surface increased to 83.7° owing to the weaker hydrophilicity of PLLA blocks [44]. The contact angle of the 5sPCL-*b*-PLLA-BSPA surface increased to 85.5°, which should be ascribed to the substitution of the terminal hydroxyl groups of the copolymer by BSPA. As for the surfaces of 5sPCL-*b*-PLLA-*b*-PDMAEMA (sample 6) and 5sPCL-*b*-PLLA-*b*-PDMAEMA (sample 10), the contact angles were 21.2° and 10.4°, respectively. This should be attributed to the presence of PDMAEMA blocks with good hydrophilicity. Therefore, the hydrophilicity of copolymers could be improved and adjusted by the alteration of the composition of the PCL, PLLA and PDMAEMA segments in copolymers. The changes of the hydrophilicity can also prove indirectly the structure and composition of copolymers composed of the hydrophobic PCL and PLLA and the hydrophilic PDMAEMA.

3.5. Micelle formation

The amphiphilic block copolymer can self-assemble to form nano-micelles in aqueous media. The insoluble block aggregates into a core that is held into solution by the outer soluble block. The core-shell structure of the micelles can be studied by NMR analyses [39]. Fig. 5 shows ^1H NMR spectra of 5sPCL-*b*-PLLA-*b*-PDMAEMA star-triblock copolymer in CDCl_3 and the micelles formed by the star-triblock copolymer in D_2O . The solvent CDCl_3 is capable of dissolving both hydrophobic and hydrophilic blocks while D_2O can only dissolve the hydrophilic PDMAEMA blocks. In CDCl_3 , all the ^1H

NMR resonances attributed to PCL, PLLA and PDMAEMA blocks were detected as shown in Fig. 5(a). However, the ^1H NMR spectrum of micelles in D_2O showed a complete loss of PCL and PLLA resonances due plausibly to suppressed molecular motion of the aggregated hydrophobic chains (Fig. 5(b)). ^1H NMR study in aqueous solution showed mainly hydrophilic PDMAEMA signals but not hydrophobic blocks signals, indicating a stable core-shell micellar structure with a hydrophobic viscous inner core and a hydrophilic shell [45].

3.6. Thermal-responsive behaviours of copolymer micelles

To determine whether the 5sPCL-*b*-PLLA-*b*-PDMAEMA micelles exhibit a thermal sensitivity as expected, we examined the optical transmittance of a copolymer micelle aqueous solution as a function of temperature. Fig. 9 represents typical transmittance against temperature curves for the synthesized copolymer 5sPCL-*b*-PLLA-*b*-PDMAEMA, which shows the temperature dependence of optical transmittance at 500 nm for 5sPCL-*b*-PLLA-*b*-PDMAEMA micelles in aqueous solution. With increasing of temperature, the solution can be found to be transformed from transparent to opaque gradually. In the lower temperature range (30–43 °C), the optical transmittance decreases only slightly. In contrast, the optical transmittance decreases drastically in the temperature range of 43–53 °C. The turning point appears to be around 48 °C. It is a typical LCST of temperature-responsive PDMAEMA blocks. Whilst the PCL-*b*-PLLA blocks are hydrophobic, the PDMAEMA blocks are hydrophilic at ambient temperature and become hydrophobic above the demixing temperature as a result of the lower critical solution temperature (LCST) behavior [46]. The visual illustration of the optical transmittance changes is illustrated on the enclosed photographs in Fig. 9, where clear and turbidity dispersions are observed upon reversible cooling and heating cycles of the copolymer aqueous solution.

3.7. pH-responsive behaviours of copolymer micelles

In order to determine pH responsiveness of the copolymer micelles, the optical transmittance and particle size of copolymer micelles in aqueous solution was analyzed as a function of pH at

ambient temperature. Fig. 10 illustrates pH dependence of optical transmittance at 500 nm for aqueous 5sPCL-*b*-PLLA-*b*-PDMAEMA solution. As seen, with the increase of pH value, the solution was transformed from transparent to opaque gradually, indicating the obvious pH-responsive property of PDMAEMA blocks. The enclosed photographs in Fig. 10 has provided a better overview of the optical transmittance changes with reversible increasing and decreasing pH values of the copolymer aqueous solution. DLS was used to measure the size of 5sPCL-*b*-PLLA-*b*-PDMAEMA micelles in aqueous solution at a concentration of 2 mg/mL at different pH values, and the results are shown in Fig. 11. The hydrodynamic radius (R_h) decreases from 119 to 76 nm as the pH values increase from 1.0 to 12.0 at ambient temperature. This behavior was attributed to the protonation/deprotonation of the tertiary amine functional groups in PDMAEMA component. At pH 1.0, the PDMAEMA chains are entirely protonated and highly stretched along the radial direction because of the geometrical constraint and the electrostatic repulsion between polymer chains. As pH changes from 1.0 to 12.0, PDMAEMA chains gradually shrink and precipitate from solution due to the deprotonation of amine groups [47,48].

3.8. Morphology of the copolymer micelles

The micelle aggregates of the amphiphilic copolymer 5sPCL-*b*-PLLA-*b*-PDMAEMA were prepared by dialysis method in aqueous media. The morphology of the micelles was examined by TEM and AFM. It can be seen from the image of Fig. 12(a) that 5sPCL-*b*-PLLA-*b*-PDMAEMA copolymers can self-assemble into stable and uniform micelles in water. AFM image (Fig. 12(b)) further confirms that the amphiphilic copolymers can form uniform spherical micelles. In addition, there seems to be a tendency that individual aggregates stick to each other in TEM image. A possible reason is that the unprotonated PDMAEMA at the shell of micelles is soft, and its T_g is close to room temperature [49], and hence it tends to act as glue during the drying process of the particles. As shown in Fig. 12, the diameters of solid copolymer micelles were in the range of 100–150 nm observed from both TEM and AFM images for the samples prepared from copolymer (sample 8) aqueous solution at pH = 7. The particle size and size distribution of copolymer micelles were also measured by DLS. The average hydrodynamic diameter (D_h) of the micelles which were prepared from 5sPCL-*b*-PLLA-*b*-PDMAEMA (sample 8) aqueous solution at pH = 7 is 170 nm with a relatively narrow size distribution. It can be seen that the average diameter measured by TEM and AFM is a little smaller than that measured by DLS in aqueous solution at 25 °C. The discrepancy in size of the micelles was attributed to the fact that DLS data directly reflects the dimension of micelles in solution, where the hydrophilic chains are well dispersed in water, although one side of the hydrophilic chain is attached to the core of micelle. However, for TEM and AFM measurement, the micelle solution was deposited onto a copper grid coated with carbon film or mica surface, where PDMAEMA chains shrank during the evaporation of water, which results in the smaller diameter. Similar difference in size as a result of different measuring techniques was also reported in the literature [45,50].

4. Conclusion

The novel star-block PCL-*b*-PLLAs and amphiphilic star-triblock PCL-*b*-PLLA-*b*-PDMAEMAs with five arms were successfully synthesized by using BIS-TRIS as core. Star-shaped 5sPCL-*b*-PLLAs with narrow weight distribution were synthesized by sequential living ROP of CL and L-LA. Then, star-shaped 5sPCL-*b*-PLLA was converted into a macro-chain transfer agent (macro-CTA) for the preparation of amphiphilic star-triblock PCL-*b*-PLLA-*b*-PDMAEMA

copolymers via RAFT. The spherical micelles with degradable core and pH/thermo-double sensitive shell had been prepared from the aqueous solutions of the amphiphilic star-shaped copolymers by dialysis method. Both pH and thermal-responsive behaviours of copolymer micelles obtained in this study were investigated. The micelle size and morphology were measured by DLS, AFM and TEM. The average diameters of copolymer nanoparticles were below 200 nm.

Acknowledgments

The authors gratefully acknowledge the financial support of the Program of Shanghai Subject Chief Scientist (No. 07XD14029) and the National Natural Science Foundation of China (No. 20804029).

References

- [1] Xue YN, Huang ZZ, Zhang JT, Liu M, Zhang M, Huang SW, et al. *Polymer* 2009;50(15):3706–13.
- [2] Lo CL, Huang CK, Lin KM, Hsiue GH. *Biomaterials* 2007;28(6):1225–35.
- [3] Wei H, Chen WQ, Chang C, Cheng C, Cheng SX, Zhang XZ, et al. *J Phys Chem C* 2008;112(8):2888–94.
- [4] Chung JE, Yokoyama M, Yamato M, Aoyagi T, Sakurai Y, Okano T. *J Control Rel* 1999;62(1–2):115–27.
- [5] Soppimath KS, Tan DCW, Yang YY. *Adv Mater* 2005;17(3):318–23.
- [6] Peng D, Zhang XH, Feng C, Lu GL, Zhang S, Huang XY. *Polymer* 2007;48(18):5250–8.
- [7] Chen WQ, Wei H, Li SL, Feng J, Nie J, Zhang XZ, et al. *Polymer* 2008;49(18):3965–72.
- [8] Meier MAR, Gohy JF, Fustin CA, Schubert US. *J Am Chem Soc* 2004;126(37):11517–21.
- [9] Mountrichas G, Mpiri M, Pispas S. *Macromolecules* 2005;38(3):940–7.
- [10] Cheng J, Ding JX, Wang YC, Wang J. *Polymer* 2008;49(22):4784–90.
- [11] Qiu LY, Bae YH. *Pharmaceut Res* 2006;23(1):1–30.
- [12] Roovers J, Zhou LL, Toporowski PM, Vanderzwan M, Iatrou H, Hadjichristidis N. *Macromolecules* 1993;26(16):4324–31.
- [13] Rao JY, Zhang YF, Zhang JY, Liu SY. *Biomacromolecules* 2008;9(10):2586–93.
- [14] Gao HF, Ke M, Matyjaszewski K. *Macromol Chem Phys* 2007;208(13):1370–8.
- [15] Zhang WD, Zhang W, Zhou NC, Cheng ZP, Zhu J, Zhu XL. *Polymer* 2008;49(21):4569–75.
- [16] Wang L, Dong CM. *J Polym Sci Part A Polym Chem* 2006;44(7):2226–36.
- [17] Yuan WZ, Tang XZ, Huang XB, Zheng SX. *Polymer* 2005;46(5):1701–7.
- [18] Stenzel MH, Davis TP. *J Polym Sci Part A Polym Chem* 2002;40(24):4498–512.
- [19] Yuan WZ, Yuan JY, Zheng SX, Hong XY. *Polymer* 2007;48(9):2585–94.
- [20] Gao HF, Matyjaszewski K. *Macromolecules* 2008;41(12):4250–7.
- [21] Breland LK, Storey RF. *Polymer* 2008;49(5):1154–63.
- [22] Altintas O, Yankul B, Hizal G, Tunca U. *J Polym Sci Part A Polym Chem* 2007;45(16):3588–98.
- [23] Vora A, Singh K, Webster DC. *Polymer* 2009;50(13):2768–74.
- [24] Galaev IY, Mattiasson B. *Trends Biotechnol* 1999;17(8):335–40.
- [25] Lu W, Zhang Y, Tan YZ, Hu KL, Jiang XG, Fu SK. *J Control Rel* 2005;107(3):428–48.
- [26] Zhang X, Li J, Li W, Zhang A. *Biomacromolecules* 2007;8(11):3557–67.
- [27] Hong HY, Mai YY, Zhou YF, Yan DY, Chen YJ. *Polym Sci Part A Polym Chem* 2008;46:668.
- [28] Sui XF, Yuan JY, Zhou M, Zhang J, Yang HJ, Yuan WZ, et al. *Biomacromolecules* 2008;9(10):2615–20.
- [29] Fournier D, Hoogenboom R, Thijs HML, Paulus RM, Schubert US. *Macromolecules* 2007;40(4):915–20.
- [30] Bütün V, Armes SP, Billingham NC. *Polymer* 2001;42(14):5993–6008.
- [31] Vamvakaki M, Unali GF, Bütün V, Boucher S, Robinson KL, Billingham NC, et al. *Macromolecules* 2001;34(20):6839–41.
- [32] Lad J, Harrison S, Mantovani G, Haddleton DM. *Dalton Trans* 2003;21:4175–80.
- [33] Wan DC, Fu Q, Huang JL. *J Polym Sci Part A Polym Chem* 2005;43(22):5652–60.
- [34] Boschmann D, Manz M, Poppler AC, Sorensen N, Vana P. *J Polym Sci Part A Polym Chem* 2008;46(21):7280–86.
- [35] Boschmann D, Vana P. *Macromolecules* 2007;40(8):2683–93.
- [36] Zhang W, Liu L, Zhuang X, Li X, Bai J, Chen Y. *J Polym Sci Part A Polym Chem* 2008;46(21):7049–61.
- [37] Kohori F, Sakai K, Aoyagi T, Yokoyama M, Sakurai Y, Okano T. *J Control Rel* 1998;55(1):87–98.
- [38] Chang C, Wei H, Quan CY, Li YY, Liu J, Wang ZC, et al. *J Polym Sci Part A Polym Chem* 2008;46(9):3048–57.
- [39] Choi C, Chae SY, Nah JW. *Polymer* 2006;47(13):4571–80.
- [40] Taromi FA, Grubisicgallot Z, Rempp P. *Eur Polym J* 1989;25(11):1183–7.
- [41] Fazeli N, Mohammadi N, Taromi FA. *Polym Test* 2004;23(4):431–5.
- [42] Gottschalk C, Frey H. *Macromolecules* 2006;39(5):1719–23.
- [43] Lee H, Chang T, Lee D, Shim MS, Ji H, Nonidez WK, et al. *Anal Chem* 2001;73(8):1726–32.
- [44] Tsuji H, Ishida T, Fukuda N. *Polym Int* 2003;52(5):843–52.

- [45] Zhu JL, Zhang XZ, Cheng H, Li YY, Cheng SX, Zhuo RX. *J Polym Sci Part A Polym Chem* 2007;45(22):5354–64.
- [46] San Miguel V, Limer AJ, Haddleton DM, Catalina F, Peinado C. *Eur Polym J* 2008;44(11):3853–63.
- [47] Plunkett KN, Moore JS. *Langmuir* 2004;20(16):6535–7.
- [48] Pantoustier N, Moins S, Wautier M, Degee P, Dubois P. *Chem Commun* 2003;3:340–1.
- [49] Gohy JF, Antoun S, Jerome R. *Macromolecules* 2001;34(21):7435–40.
- [50] Ye Q, Zhang ZC, Jia HT, He WD, Ge XW. *J Colloid Interf Sci* 2002;253(2):279–84.